は肩などにタッチされたとき，すぐに反応することができるが，短い欠神発作と区別が困難なこともある．複雑部分発作では発作後の意識朦朧状態の存在から白昼夢状態を区別しうる．しかし，ADHDでは不眠状態にあることも多く，結果として睡眠状態に陥っていることもあるので，最終的にはビデオ脳波モニターによる発作時脳波の確認が必要となる．

さらに，不注意に関して，てんかん発作波の影響も考えられる．従来，臨床的なてんかん発作症状のない脳波上にみられる発作波だけでは，薬物治療の対象にしないことが多かったが，てんかん発作波の出現時に軽度の注意状態の欠損がみられることが明らかになってきた．Aartsら[8]は，サブクリニカルな発作波の発射中に一過性の認知の途絶え（transient cognitive impairment）があることを報告している．このような状態は発作波発射の高頻度の患者では約50％にみられ，とくに3 Hz棘徐波結合でもっともよくみられ，不規則棘徐波結合や，発作性のデルタ波群発では影響は少ないといわれている．注意や想起のテストでは，発作波の部分の約1/3に，患者の2/3に一過性の認知の途絶えがみられ，この変化は全般性発作波の量の変化に対応する．また，焦点性発作波の場合には出現部位の神経心理学的脳機能に対応した変化がみられる．

しかし一方では，ADHDで高頻度に中心・側頭部に発作波を呈する率が高く，中心・側頭部に発作波を呈したこれらの症例での認知機能に差はなかったが多動性・衝動性が目立ったとの報告も見られる[9]．

3．学習障害

学習障害はDSM-Ⅳ-TRでは，①読字障害，②算数障害，③書字表出障害，④特定不能の学習障害，に分類されている．

読字障害での研究では，画像検査において微細な脳形成異常が見られるなどの報告が増加しており，脳になんらかの器質的もしくは機能的異常があって生じると考えられている．このようなことから，てんかんに学習上の問題が生じやすいことも事実である．Changら[10]は，2個以上のperiventricular nodular heterotopia（PNH）と，てんかんをもった10例についてMRIと神経心理学的に検討し，10例中8例に正常知能にかかわらず，読みの障害がみられたとしている．障害の程度が強かった例では，より広くPNHが分布しており，てんかんの重症度や薬剤使用とは関係がなかった．

てんかん児の中に学習障害をおこす児がどの程度存在するかについて，小児期発症の成人てんかん患者について検討したところ，約37％に学習障害がみられ，そのうち正常知能（IQ＞85）の中では57％，境界知能では67％にみられた．症候性の病因が学習障害の予知因子であり，学習障害の存在は医学的，社会的および学習の予後に影響していた[11]．

Vinayanら[12]は，中心・側頭部に棘波をもつ良性小児てんかん（BECCT）50例について検討し，教育上の問題が27例，54％にみられ，そのうち19例に学習障害をうかがわせる神経心理学的な異常があり，教育上の問題と神経心理学的な異常との間には明らかな関係があったとしている．棘波の双極子について検討し，典型的な前頭部陽性，中心・側頭部陰性で前頭・中心部にまたがる接線方向の双極子をもったものでは教育上の問題が少なく，そうでないものでは非典型的な発作が多く，教育上の問題も多かった．

発達性計算障害は未熟児，低出生体重児におこりやすく，ADHD，てんかん，発達性の言語障害などとの合併もみられ，左側頭頭頂葉領域の機能がとくに重要であるが，正常の数学的スキルに必要な両半球の神経ネットワークの機能も関係する．このようにてんかん焦点の局在と学習障害との関連について，側頭葉てんかんでは，和田テストで左半球優位であったもので読

表 3

ガイドラインA案（普通学級用）（文献14）より引用）

てんかん患児管理指導表

所見名（診断名）　　平成　　年　　月　　日

学校名　　医療機関

氏　名　　医師　　㊞

管理区分決定のめやす 発作の頻度・強度からの分類	発作強度	
	弱	強
発作頻度	短時間の意識消失，程度の軽いけいれん発作など	外傷の危険が大きい，転倒を伴う，けいれん後も意識消失が長びく発作など
1回/日程度以上	B	A
1回/週程度以上	C	B
1回/月程度以上	C	B
1～2回/年程度	C	C
1年以上発作なし	D	C
3年以上発作なし	E	E

学校生活の区分	教室内学習	体水育泳実を技除く	水泳	部活動
A	要注意	1対1などの厳重注意		
B	注意して可	要注意（監視が必要）		
C	可	注意して可	要注意	注意して可
D	可		注意して可	可
E	可			

学校行事，その他の活動

Ⅰ．児童生徒活動：Aは厳重注意，Bは要注意，C・Dは可
Ⅱ．食事当番・清掃：Aは厳重注意，Bは要注意，C・Dは可
Ⅲ．朝会やその他の集会：Aは厳重注意，Bは要注意，C・Dは可
Ⅳ．運動会，体育祭，球技大会：Aは厳重注意，Bは要注意，C・Dは可
Ⅴ．水泳大会，臨海学校：Aは厳重注意，B・Cは要注意，Dは必要により何らかの対策をとる必要がある
Ⅵ．遠足，見学，移動教室：Aは厳重注意，Bは要注意，C・Dは可
Ⅶ．林間学校，修学旅行：Aは厳重注意，Bは要注意，C・Dは服薬が医師の指示通り行われることが必要

区分Cは「可」であっても，場合により監視が必要．区分Dの水泳は，必要により何らか対策をとる必要がある

ガイドラインB案（特殊学級，養護学校用）（文献14）より引用）

頻度区別・強度	教室内学習	体育実技（除く水泳）	水泳	部活動	児童活動	給食清掃当番	朝会・集会	球運技動大会会	移遠動教室足	林修間学学旅校行	林間学校
A	1対1などの厳重注意が必要										
B	監視下であれば可（厳重に監視）										
C	監視下であれば可（注意して監視）										
D	可		可*	可							可*
E	可										

*：必要により何らかの対策をとる必要がある

み理解，書き，計算の能力障害のあるものの，頻度は左側頭葉に焦点のあるもので高率で75％以上であった．逆に右焦点では10％未満であった．すなわち，優位半球でのてんかんの発症は，学習障害の頻度が高くなることが予見される[13]．

てんかん児の保育所・幼稚園・学校生活について

1．スポーツ，課外活動，その他

てんかん児の学校でのスポーツや課外活動については原則参加の方向であるが，保護者が学校に病名を伝えているかどうかが問題になってくる．伝えていない場合には，この原則は当てはまらない．学校への病名告知は理想であるが，現実にはさまざまな問題があり躊躇せざるをえないこともある．しかし，発作頻度が比較的高いときには告知せざるをえないと思われる．学校行事への参加に関して，厚生労働省心身障害研究「小児慢性疾患のトータルケアに関する研究」（1992）によるガイドラインが参考になる[14]（表3）．

Wongらは[15]，てんかん児の生活活動について調査してんかんでない同胞と比較した．てんかん児では同胞より活動性が少なく，肥満気味であった．とくに，3剤以上の抗てんかん薬を服用している児ではスポーツに関与することが少なく，発作頻度が関係することがうかがわれたが，スポーツにかかわることでの発作関連のけが，発作自体はスポーツへのかかわりに関係なかったとし，運動を奨励するプログラムが推進されるべきであるとしている．発作の児童の運動への関与は精神的にもよく，社会性，自尊心を高め，自己肯定感を育て，QOLを改善する効果があると考えられる．また，過度ではない精神的な高揚は覚醒度を上げ，発作を抑制する効果もある．

2．予防接種

1994年に予防接種法が改正され，てんかんのある子どもでも現行の予防接種を行えるようになった．同年予防接種ガイドラインが出され，その後何度か改められてきた．2005年の予防接種ガイドラインによるとてんかんの既往のある者に対しての基準が示されている[16]（表4）．

集団生活になると感染症に罹患し発熱する機会が増え，てんかんや熱性けいれんのある子どもでは，けいれんが誘発されることも多い．と

表4　てんかん既往者の予防接種基準（2005年予防接種ガイドライン）

1. コントロールが良好なてんかんを持つ小児では，最終発作から2～3カ月程度経過し，対朝が安定していれば現行のすべてのワクチンを接種しても差し支えない
2. 1．以外のてんかんを持つ小児においてもその発作状況がよく確認されており，症状と体調が安定していれば主治医（接種医）が適切と判断した時期にすべての予防接種をしても差し支えない
3. 発熱によって痙攣発作が誘発されやすいてんかん児（重症ミオクロニーてんかんなど）では，副反応による発熱が生じた場合の発作予防策（ジアゼパム坐剤，経口剤など）と万一発作時の対策を指導しておく
4. ACTH療法後のワクチンは6カ月以上あけて接種する（＊）
5. ガンマグロブリン大量療法（総投与量が約1 g/kg以上）後の生ワクチン（風疹，麻疹，水痘，ムンプスなど）は6ヶ月以上，それ以外の量では3カ月以上あけて接種する（＃）．ただし，接種効果に影響がないワクチン（ポリオ，BCG，DPT，インフルエンザなど）はこの限りでない
6. なお，いずれの場合も事前に保護者への十分な説明と明示の同意が必要である

＊：ACTH後の免疫抑制状態における生ワクチン接種による罹患と抗体獲得不全のリスクは，ACTH投与量，投与方法で差があるので主治医（接種医）の判断でこの時期は変更可能である

＃：接種前3カ月以内に輸血又はガンマグロブリン製剤の投与を受けた者は，本剤の効果が得られない恐れがあるので，3カ月以上過ぎるまで摂取を延期すること．また，ガンマクログロブリン製剤の大量療法，すなわち川崎病，特発性血小板減少性紫斑病（ITP）等の治療において200 mg/kg以上投与を受けた者は，6カ月以上（麻疹感染の危険性が低い場合は11カ月以上）過ぎるまで接種を延期すること

くに，発熱によりけいれん重積になりやすい乳児重症ミオクロニーてんかんでは注意が必要である．このようなことから，各予防接種の副反応の特徴を把握し，とくに発熱時のけいれんに対する万全の対応をとって，積極的に予防接種を行うべきであろう．保護者や本人に予防接種の目的，意義，予想される副反応などについて十分に説明し，納得を得るとともに，発熱，けいれん時の対応を指導する．発熱に気づいたときにはジアゼパムを用いる．坐剤または経口的に 0.4 ～ 0.5 mg/kg/回（最大 10 mg/1 回），発熱持続時は 8 時間後 0.3 ～ 0.4 mg/kg/回（最大 10 mg/回）を追加する．

●文　献

1) Kobayashi R, Murata T, Yoshinaga K: A follow up study of 201 children with autism in Kyushu and Yamaguchi area. J Autism Dev Disord 22: 395-411, 1992
2) Danielsson S, Gillberg IC, Billstedt E et al.: Epilepsy in young adults with autism: a prospective population-based follow-up study of 120 individuals diagnosed in childhood. Epilepsia 46: 918-923, 2005
3) Clarke DF, Roberts W, Daraksan M et al.: The prevalence of autistic spectrum disorder in children surveyed in a tertiary care epilepsy clinic. Epilepsia 46: 1970-1977, 2005
4) 川崎葉子：広汎性発達障害とてんかん．発達障害医学の進歩 18 集，診断と治療社，東京，39-49, 2006
5) Hashimoto T, Sasaki M, Sugai K et al.: Paroxysmal discharges on EEG in young autistic patients are frequent in frontal regions. J Med Invest 48: 175-180, 2001
6) Chez MG, Chang M, Krasne V et al.: Frequency of epileptiform EEG abnormalities in a sequential screening of autistic patients with no known clinical epilepsy from 1996 to 2005. Epilepsy Behav 8; 267-271, 2006
7) Hesdorffer DC, Ludvigsson P, Olafsson E et al.: ADHD as a risk factor for incident unprovoked seizures and epilepsy in children. Arch Gen Psychiatry 61: 731-736, 2004
8) Aarts JHP, Binnie CD, Smith AM et al.: Selective cognitive impairment during focal and generalized epileptiform EEG activity. Brain 107: 293-308, 1984
9) Schubert R: Attention deficit disorder and epilepsy. Pediatr Neurol 32: 1-10, 2005
10) Chang BS, Ly J, Appignani B et al.: Reading impairment in the neuronal migration disorder of periventricular nodular heterotopia. Neurology 64: 799-803, 2005
11) Sillanpaa M: Learning disability: occurrence and long-term consequences in childhood-onset epilepsy. Epilepsy Behav 5: 937-944, 2004
12) Vinayan KP, Biji V, Thomas SV: Educational problems with underlying neuropsychological impairment are common in children with benign epilepsy of childhood with centrotemporal spikes (BECTS). Seizure 14: 207-212, 2005
13) Butterbaugh G, Olejniczak P, Roques B et al.: Lateralization of temporal lobe epilepsy and learning disabilities, as defined by disability-related civil rights law. Epilepsia 45: 963-970, 2004
14) 前澤眞理子，関　亨，木実谷哲史・他：日常生活のアドバイス．小児内科 34: 822-826, 2002
15) Wong J, Wirrell E: Physical activity in children/teens with epilepsy compared with that in their siblings without epilepsy. Epilepsia 47: 631-639, 2006
16) 予防接種ガイドライン等検討委員会：予防接種ガイドライン．財団法人予防接種リサーチセンター，2005

著者連絡先

〒772-8502　徳島県鳴門市鳴門町高島字中島 748
鳴門教育大学障害児教育講座
橋本俊顕

R. Okamoto[1]
S. Fujii[2]
T. Inoue[1]
K. Lei[1]
A. Kondo[1,3]
T. Hirata[4]
M. Okada[4]
I. Suzaki[5]
T. Ogawa[2]
Y. Maegaki[1]
K. Ohno[1]

Biphasic Clinical Course and Early White Matter Abnormalities may be Indicators of Neurological Sequelae after Status Epilepticus in Children

Original Article

Abstract

Clinical course and serial neuroimaging findings are not fully described in children who have had neurological sequelae following status epilepticus. We found four patients who had neurological sequelae out of 42 children with status epilepticus in 2004. MRI studies were reviewed with specific attention to diffusion-weighted images (DWI) and the apparent diffusion coefficient (ADC). Proinflammatory cytokines, including tumor necrosis factor-α and interleukin-6, were measured in the cerebrospinal fluid (CSF) (3 patients). The clinical course showed biphasic; initial status epilepticus and neurological exacerbation along with seizure recurrence four to five days after onset. Within three days after initial status epilepticus, CT (all patients) and MRI (2 patients) did not show any abnormalities. From four to ten days after onset, MRI demonstrated diffuse hyperintensity in the cerebral white matter on DWI and hypointensity on ADC maps in all patients. Diffuse brain atrophy progressed thereafter. Tumor necrosis factor-α or interleukin-6 was elevated in all patients. A biphasic clinical course may be a specific feature for neurological sequelae. The preferential white matter involvement on MRI and elevated CSF cytokines indicate that glial dysfunction may play an important role in the pathophysiology of status epilepticus-associated cerebral damage.

Key words
Status epilepticus · children · diffusion-weighted images · ADC maps · white matter · biphasic clinical course

Abbreviations

ADC	apparent diffusion coefficient
CSF	cerebrospinal fluid
DWI	diffusion-weighted image
EEG	electroencephalogram
FLAIR	fluid-attenuated inversion recovery
IL-6	interleukin-6
IV	intravenous
SE	spin-echo
TE	echo time
T_1WI	T_1-weighted image
T_2WI	T_2-weighted image
TNF-α	tumor necrosis factor-alpha
TR	repetition time

Affiliation
[1] Division of Child Neurology, Institute of Neurological Sciences, Faculty of Medicine, Tottori University, Yonago, Japan
[2] Division of Radiology, Institute of Neurological Sciences, Faculty of Medicine, Tottori University, Yonago, Japan
[3] Department of Pediatrics, Tottori Prefectural Central Hospital, Tottori, Japan
[4] Department of Pediatrics, Matsue Red Cross Hospital, Matsue, Japan
[5] Department of Pediatrics, Tottori Prefectural Kousei Hospital, Kurayoshi, Japan

Correspondence
Yoshihiro Maegaki · Division of Child Neurology, Institute of Neurological Sciences · Faculty of Medicine · Tottori University · 36 – 1 Nishi-Cho · Yonago 683 – 8504 · Japan ·
E-mail: maegaki@grape.med.tottori-u.ac.jp

Received: September 6, 2005 · **Accepted after Revision:** January 27, 2006

Bibliography
Neuropediatrics 2006; 37: 32 – 41 © Georg Thieme Verlag KG Stuttgart · New York ·
DOI 10.1055/s-2006-923949 ·
ISSN 0174-304X

Introduction

Status epilepticus is a common emergency in infants and children and poses a risk for status epilepticus-associated neurological sequelae. Neurological sequelae following status epilepticus have reached 10–20% in recent pediatric series [17,25]. Although there have been many imaging studies dealing with cerebral abnormalities during or following status epilepticus, these were mostly evaluated by conventional CT or MRI, including T_1-weighted images (T_1WI), T_2-weighted images (T_2WI), and fluid-attenuated inversion recovery (FLAIR) images. Cerebral abnormalities associated with status epilepticus usually show hypointensity on CT, hyperintensity on T_2WI and FLAIR image, indicating cerebral edema. A recent advantage of neuroimaging revealed that diffusion-weighted images (DWI) and the apparent diffusion coefficient (ADC) are more sensitive in identifying ischemic cerebral lesions than conventional MRI. DWI and ADC reflect changes in water diffusion and appear useful in distinguishing between cytotoxic edema and vasogenic edema. In the acute stage of ischemic cerebral lesion, hyperintensity on DWI and hypointensity on the ADC map means cytotoxic edema, which is usually followed by cerebral atrophy. Instead, isointensity on DWI despite hyperintensity on T_2WI and FLAIR image means vasogenic edema, which is usually reversible. Therefore, DWI and ADC are superior in identifying cerebral abnormalities and evaluating the pathophysiology of cerebral abnormalities than the conventional neuroimaging. DWI and ADC have been applied in patients with status epilepticus [1,3,4,6,7,9,10,12–15,27]. Researchers have successfully demonstrated cerebral abnormalities similar to ischemia: hyperintensity on DWI and hypointensity on ADC maps were also shown in the epileptogenic area. MRI abnormalities were predominantly located in the gray matter and were mostly transient and reversible [6,12,14,15,27]. Therefore, the gray matter is considered to be more vulnerable to status epilepticus. We report four patients who suffered status epilepticus and developed neurological sequelae, and showed prominent white matter abnormalities on DWI and ADC maps several days after status epilepticus.

Patients and Methods

Study population and design

Tottori University Hospital, Tottori Prefectural Central Hospital, Tottori Prefectural Kousei Hospital, and Matsue Red Cross Hospital serve the whole area of Tottori Prefecture and the eastern part of Shimane Prefecture. All emergency cases of infants and children in this area are referred to these four hospitals. We reviewed the medical records of infants and children aged 1 month to 16 years who were referred to any of these hospitals due to status epilepticus from January to December in 2004. Status epilepticus was defined as any seizure lasting more than 30 minutes or recurrent seizures lasting a total of more than 30 minutes without complete recovery of consciousness. We excluded patients who had status epilepticus due to an acute symptomatic cause such as meningitis, encephalitis, head trauma, cerebrovascular disease, and systemic and metabolic disease. We also excluded patients with specific encephalopathy such as Reye's syndrome, acute necrotizing encephalopathy, and hemorrhagic shock and encephalopathy. The reason is that pathophysiological changes other than status epilepticus strongly affect cerebral injury in these diseases. To identify the possible causes of status epilepticus, a routine laboratory examination including a complete blood count, blood chemistry, serum glucose, urinalysis, cerebrospinal fluid (CSF), cranial CT or MRI, and EEG was performed for each patient. Further metabolic analysis including plasma and urine amino acids, urine organic acids, and blood and CSF lactic acids was performed in patients who showed any neurological sequelae after status epilepticus.

Data acquisition

CT and MRI were reviewed by neuroradiologists (SF, TO). MRI was performed on a 3-T system (Signa Horizon; GE Medical Systems, Milwaukee, WI, USA) or 1.5-T systems (EXCELART, Toshiba, Tokyo, Japan and Signa, GE Medical Systems, Milwaukee, WI, USA). T_1WIs were obtained by the spin-echo (SE) technique with a repetition time (TR) of 450–460 msec and an echo time (TE) of 11–12 msec (450–465/11–12) on the 1.5-T systems. On the 3-T, T_1WIs were obtained by 3D RF-spoiled gradient echo (SPGR) with 9/2/18 (TR/TE/flip angle). T_2WIs were obtained by using a fast SE technique with 4000–4200/83.5–101 (TR/TE). FLAIR images were obtained with 8002–10 002/110–120/1800–2500 (TR/TE/inversion time). Single-shot DWI was performed in the axial projection with 5999–7000/84–110 (TR/TE), low-strength gradient (b: 0 sec/mm^2), and high-strength diffusion gradient (b: 1000 sec/mm^2). The low b value images served as a baseline for comparison with the high b value images. These images were obtained by varying diffusion gradient strength along each of three orthogonal directions. Diffusion trace maps were computed from the isotropic diffusion image. ADC maps were calculated on the basis of these b0 and b1000 images.

Cytokine assay

Interleukin-6 (IL-6) and tumor necrosis factor–alpha (TNF-α) were measured in CSF using the human chemiluminescent immunoassay kits by R&D systems (Minneapolis, MN, USA). CSF samples were collected from three patients (Patients 1, 2, and 4) after the elimination of initial status epilepticus. A CSF sample was also taken on the fourth day of onset in Patient 1. The normal range of CSF TNF-α was less than 6.2 pg/mL and that of IL-6 was less than 9.7 pg/mL [11].

Results

Fifty status epilepticus episodes in 42 children met the inclusion criteria for the present study. Diagnosis was febrile convulsion for 23 episodes in 23 children, and epileptic seizure for 27 episodes in 19 children. We found four patients who suffered status epilepticus followed by neurological sequelae out of 23 patients with febrile convulsion.

Case reports

Patient 1

A 19-month-old boy was born by Cesarean section due to Chiari malformation. Myelomeningocele and hydrocephalus were recognized and surgical repair was performed early after birth. He required placement of a ventriculoperitoneal shunt at two months of age. His mental and motor development were mildly delayed at 18 months. He had no previous seizures. The patient

was referred to the hospital due to pyrexia for three days and then presented with generalized clonic convulsions. His seizure continued for 25 minutes despite rectal and intravenous (IV) administration of diazepam and IV midazolam. It was ameliorated with IV thiopental but recurred soon. Clinical seizure was then stopped with repeated use of thiopental, while ictal EEG discharges continued in the right occipital region. EEG seizure activity was eventually stopped with rectal administration of phenobarbital. The observed seizure duration including clinical and EEG seizures was 180 minutes.

On admission he was unresponsive with a body temperature of 39.7 °C. Physical examination was unremarkable except for respiratory distress. He showed no meningeal signs. Routine laboratory tests revealed a leukocyte count of 12900/μL and serum CRP levels of 4.0 mg/dL. Other routine laboratory findings were unremarkable. CSF examination was normal. Viral and bacterial cultures were negative in CSF. Metabolic analysis was unremarkable. CT findings were unchanged compared to the previous studies. Sleep EEG showed continuous slow waves in the occipital region. Rectal administration of phenobarbital was maintained to prevent recurrence of seizure. When he became afebrile on the third day of seizure onset, he was still in a semicoma, but sometimes opened his eyes and followed his parent's movements with his eyes. He showed severe hypotonia. A few series of apnea were found. Routine laboratory tests, CSF examination and EEG were repeated and were all unremarkable.

Brief but frequent partial seizures recurred on the fifth day of onset. The seizure was not controllable only with IV thiopental but stopped with continuous IV infusion of midazolam. After the seizure recurrence, he went into a coma and developed choreoathetoid movements bilaterally. A year later, the patient was able to control his head, but was not able to sit without support or speak.

Patient 2

A 13-month-old boy was referred to the hospital due to status epilepticus. He had no previous seizures or neurological illness. His birth was uneventful and his development was normal. His father had febrile convulsions in childhood. He had febrile illness and generalized tonic-clonic convulsions occurred on the same day. When he reached the hospital, his seizure continued for 120 minutes despite a rectal administration of diazepam. IV diazepam and midazolam failed to stop the seizure but it was eventually controlled with IV thiamylal. The clinically observed seizure duration was 150 minutes. On admission, he was unresponsive with a body temperature of 40.6 °C. Physical examination was unremarkable except for respiratory distress. He showed no meningeal signs. Routine laboratory findings were all unremarkable. CSF examination was also normal. Viral and bacterial cultures were negative in CSF. Metabolic analysis was unremarkable. Cranial CT and MRI were unremarkable. Sleep EEG was also unremarkable on the second day. A continuous IV of midazolam and rectal administration of phenobarbital were maintained to prevent recurrence of seizure. On the second day of onset, he was in a semicoma, but sometimes opened his eyes and followed his parent's movements with his eyes. Status epilepticus recurred on the fourth day of onset. The seizure was not controllable only with IV diazepam and midazolam but stopped with continuous IV infusion of thiamylal. After the second status epilepticus, he went into a deep coma. Sleep EEG showed generalized slow waves. When he became afebrile on the sixth day of onset, a small skin rash appeared. Human herpes virus-6 DNA was isolated from the blood by PCR, but not from the CSF. Therefore he was diagnosed with exanthema subitum. The patient then developed choreoathetoid movements bilaterally. A year later, he was able to sit without assistance and follow an object with his eyes, but was not able to walk or reach an object with his hands. He had subtle but daily seizures.

Patient 3

An 18-month-old girl was referred to the hospital due to status epilepticus. She had no previous seizures or neurological illness. Her birth was uneventful and her development was normal. Her uncle had febrile convulsions in childhood. She had febrile illness and right hemi-convulsion on the same day. When she reached the hospital, her seizure continued for 60 minutes despite rectal administration of diazepam. Her seizure was ameliorated with IV diazepam but recurred soon, and was eventually controlled with IV midazolam. The clinically observed seizure duration was 90 minutes. On admission she was unresponsive with a body temperature of 39.3 °C. Physical examination was unremarkable except for respiratory distress. She had motor palsy in the right upper and lower extremities. She showed no meningeal signs. Routine laboratory findings were all unremarkable. CSF examination was also normal. Viral and bacterial cultures were negative in CSF. Metabolic analysis was unremarkable. Cranial CT was unremarkable. IV midazolam and rectal administration of phenobarbital were maintained to prevent recurrence of seizure. On the second day of onset, she was in a semicoma, but sometimes she opened her eyes and followed her parent's movements with her eyes. She showed hemiparesis and hemianopsia on the right side. On the fourth day of onset, she went into a deep coma and MRI abnormalities were evident. Repetitive clonic convulsions of the right side of the body recurred on the fifth day of onset. The seizure was not controllable with IV midazolam and phenytoin but was stopped with continuous IV infusion of thiamylal. She then developed transient tremorous movements bilaterally. A year later, she was severely mentally retarded with right hemiparesis and right hemianopsia, and intractable epilepsy. She was able to sit without assistance and follow an object with her eyes, but was not able to walk or reach an object with her hands.

Patient 4

A 12 month-old boy was referred to the hospital due to status epilepticus. He had no previous seizures or neurological illness. His birth was uneventful and his development was normal. He had febrile illness and generalized tonic-clonic convulsion occurred on the next day. When he reached the hospital, his seizure continued for 120 minutes despite IV administration of diazepam. The seizure was eventually controlled with the additional usage of diazepam and phenobarbital. The seizure duration ultimately reached 150 minutes. On admission he was unresponsive with a body temperature of 39 °C. He showed no meningeal signs. Routine laboratory findings were all unremarkable. CSF leukocyte count was 16/mm^3 (33% polynuclear leukocytes and 67% mononuclear leukocytes) and normalized on the next day. Viral and bacterial cultures were sterile in CSF. Metabolic analysis was un-

Table 1 Summary of CT and MRI findings

	Hyperacute (days 1–3)	*Acute (days 4–10)*	*Subacute (days 11–30)*	*Chronic (day 31 onwards)*
Clinical state	semicoma	deep coma, seizure recurrence	improving	improving, mental retardation
Global CT/MRI findings	unremarkable (4/4)	mild brain swelling (4/4)	diffuse brain atrophy (4/4)	progressive atrophy (3/3)
CT	unremarkable (4/4)	loss of gray-white junction (3/3), diffuse low density (2/3)	loss of gray-white junction (2/3), diffuse low density (2/3)	
T_2WI/FLAIR	unremarkable (2/2)	linear hyperintensity in the gray-white junction (3/4) Diffuse cortical hyperintensity (2/4)	→ resolved(3/3); diffuse cortical hyperintensity (2/3) localized hyperintensity (3/3) (gray matter 1, white matter 2)	diffuse cortical hyperintensity (1/2) localized cortical hyperintensity(1/2)
Restricted diffusion on DWI and ADC maps	none (2/2)	white matter (4/4, diffuse 2, subcortical 2)	→ resolved (3/3), gray matter (localized, 1/3)	none (2/2)

remarkable. CT showed no abnormal findings. EEG demonstrated generalized slow waves. Rectal administration of phenobarbital was maintained to prevent recurrence of seizure. On the second day of onset, he was in a semicoma, but sometimes opened his eyes and followed his parent's movements with his eyes. The patient went into a coma on the fourth day of onset and the seizure recurred on the fifth day of onset. The generalized or focal clonic seizures repeated despite initiation of phenytoin and carbamazepine and eventually stopped on the next day. Six months later, when he was 18 months old, he was able to sit alone, but was not able to walk or speak. His developmental quotient was 46.

Imaging findings

CT and MRI were analyzed at different stages following status epilepticus. The hyperacute stage was within three days after the onset of status epilepticus. All patients gradually improved following status epilepticus but were still in a semicoma in this stage. CT was performed just after cessation of status epilepticus in all patients. MRI was performed in two patients. The acute stage was from the fourth to the tenth day of onset. All patients went into a deep coma and had a recurrence of seizures in this stage. MRI was performed on all patients. The subacute stage was from the 11th to the 30th day of onset. All patients started to improve after exacerbation in this stage. The chronic stage was after the 30h day of onset. All patients were still improving but neurological sequelae were evident in this stage. The changes of ADC values were examined in Patient 1. Table **1** shows a summary of the neuroimaging findings.

Patient 1

Hyperacute stage (Fig. **1A**): Neither brain swelling nor abnormal signal suggesting status epilepticus was found on CT (day 1) and MRI (day 3).

Acute stage (Fig. **1B**): CT (day 5) showed loss of gray-white junction diffusely in the cerebrum. MRI (day 7) showed gyral swelling and subtle linear hyperintensity in the gray-white junction on T_2WI and FLAIR image. DWI revealed symmetrical hyperintensities in the cerebral white matter, whereas such abnormalities were not conspicuous on T_2WI and FLAIR images. ADC maps showed restricted diffusion in the cerebral white matter.

Subacute stage (Fig. **1C**): Enlargement of the lateral ventricle and widening of the cortical sulci suggesting diffuse brain atrophy were present. Diffuse white matter hyperintensities disappeared on DWI (day 22). Hyperintensities in the bilateral occipital white matter became conspicuous on FLAIR images. Their adjacent gray matter appeared mildly hyperintense on DWI. The ADC maps showed restricted diffusion in the corresponding occipital gray matter.

Chronic stage: On the 2-month follow-up CT, progressive brain atrophy was clear as compared with images of the subacute stage.

Changes of ADC values ($\times 10^{-3}$ mm^2/s): The ADC values of the frontal gray matter at the hyperacute, acute, and subacute stages were 1.13, 1.05, and 1.23, respectively. Those of the frontal white matter were 0.80, 0.31, and 0.81, respectively. The ADC values of the occipital gray matter were 1.06, 0.83, and 0.74, respectively. Therefore, the decrease of the ADC values was 61% in the frontal white matter at the acute stage and 30% in the occipital gray matter at the subacute stage.

Patient 2

Hyperacute stage (Fig. **2A**): CT (days 1 and 3) showed no abnormal findings. Neither brain swelling nor abnormal signal intensity was found in any MR image (day 2).

Acute stage (Fig. **2B**): T_2WI and FLAIR image (day 6) showed blurring of the gray-white junction in the cerebral hemisphere, especially in the frontal lobe. Extensive gyral hyperintensity and subtle linear hyperintensity in the gray-white junction were also observed. DWI clearly revealed symmetrical hyperintensities in the periventricular and subcortical white matter. The ADC maps showed restricted diffusion in these areas. Gyral swelling was not found.

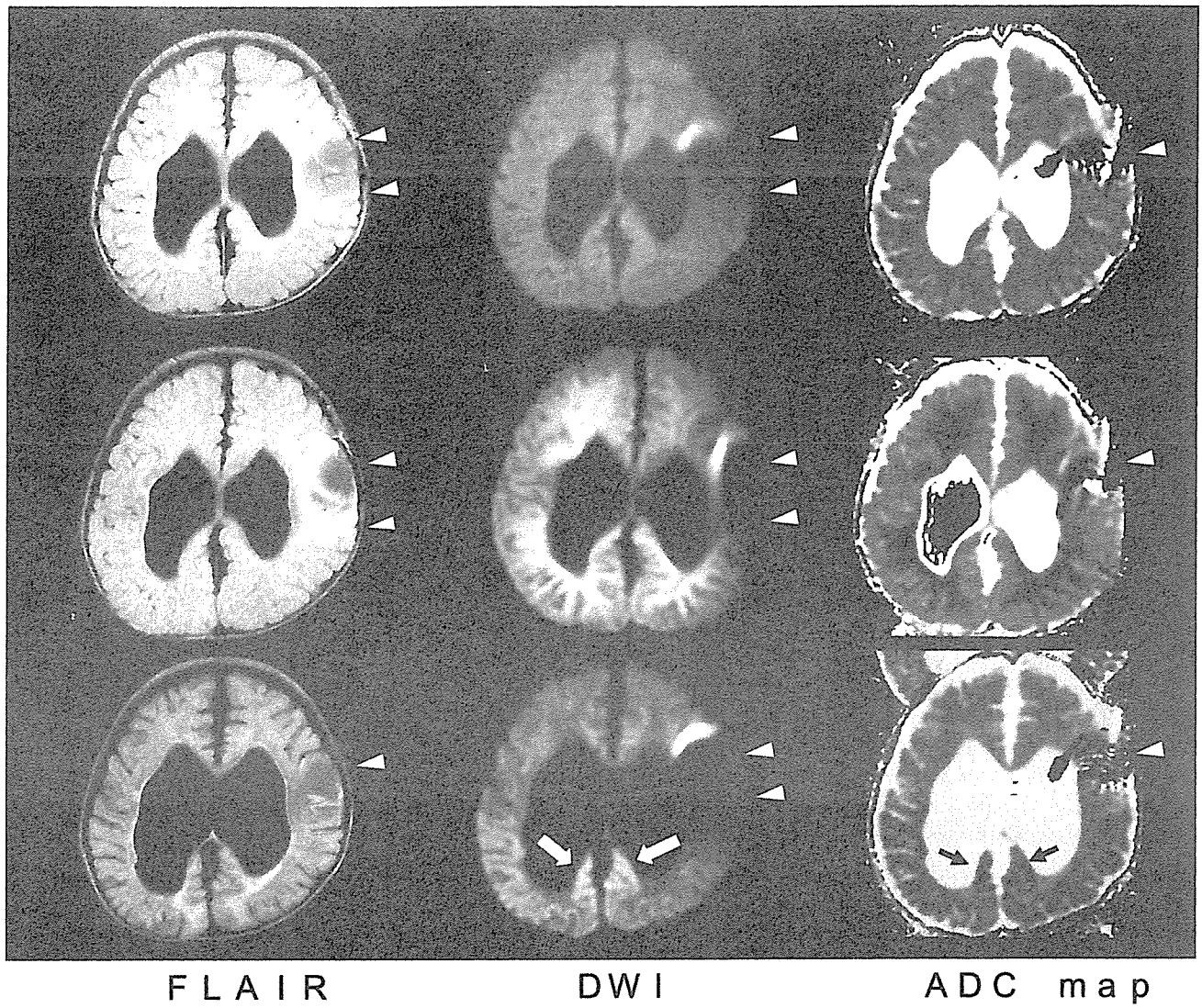

Fig. **1** Fluid-attenuated inversion recovery (FLAIR) images, diffusion-weighted images (DWI), and apparent diffusion coefficient (ADC) maps of Patient 1 at the hyperacute (**A**), acute (**B**), and subacute stages (**C**) following status epilepticus. Significant dilatation of lateral ventricles due to Chiari malformation can be seen on all MRIs. (**A**) Neither brain swelling nor abnormal signal intensity is found in the hyperacute stage. (**B**) Cerebral white matter shows symmetrical hyperintensities on DWI and hypointensities on ADC maps in the acute stage. (**C**) White matter hyperintensities disappeared on DWI and diffuse brain atrophy progressed in the subacute stage. Bilateral occipital gray matter shows mild hyperintensities on DWI and hypointensities on ADC map (arrow). A shunt valve artifact is seen in the left frontoparietal region (arrowhead).

Subacute stage (Fig. **2C**): MRI (day 15) showed mild diffuse brain atrophy. Diffuse white matter hyperintensities disappeared on DWI. DWI also showed mild hyperintensity in the left temporo-occipital region. However, restricted diffusion was not apparent in this area on the ADC maps.

Chronic stage (Fig. **2D**): T_2WI and FLAIR images showed progression of marked brain atrophy and localized periventricular hyperintensity on the 1-month follow-up MRI. FLAIR image and DWI showed mild hyperintensity of the cerebral cortices.

Patient 3

Hyperacute stage: CT (day 1) showed no abnormal findings.

Acute stage (Fig. **3A**): MR images (day 4) showed diffuse swelling of the left cerebral hemisphere. Subtle linear hyperintensity was also seen in the gray-white junction on T_2WI and FLAIR images. While mild hyperintensities in the periventricular and subcortical white matter were recognized on T_2WI and FLAIR images, these abnormalities were more conspicuous on DWI. The ADC maps showed restricted diffusion in these areas.

Subacute stage (Fig. **3B**): MR images (day 26) showed moderate diffuse brain atrophy and residual hyperintensities in the subcortical and periventricular white matter of the left temporal, parietal, and occipital lobes on the T_2WI and the DWI. The ADC maps also showed hyperintensities in the corresponding areas. Hyperintensity on DWI in these areas was due to T_2 shine-through.

Chronic stage: MR and CT images were not available.

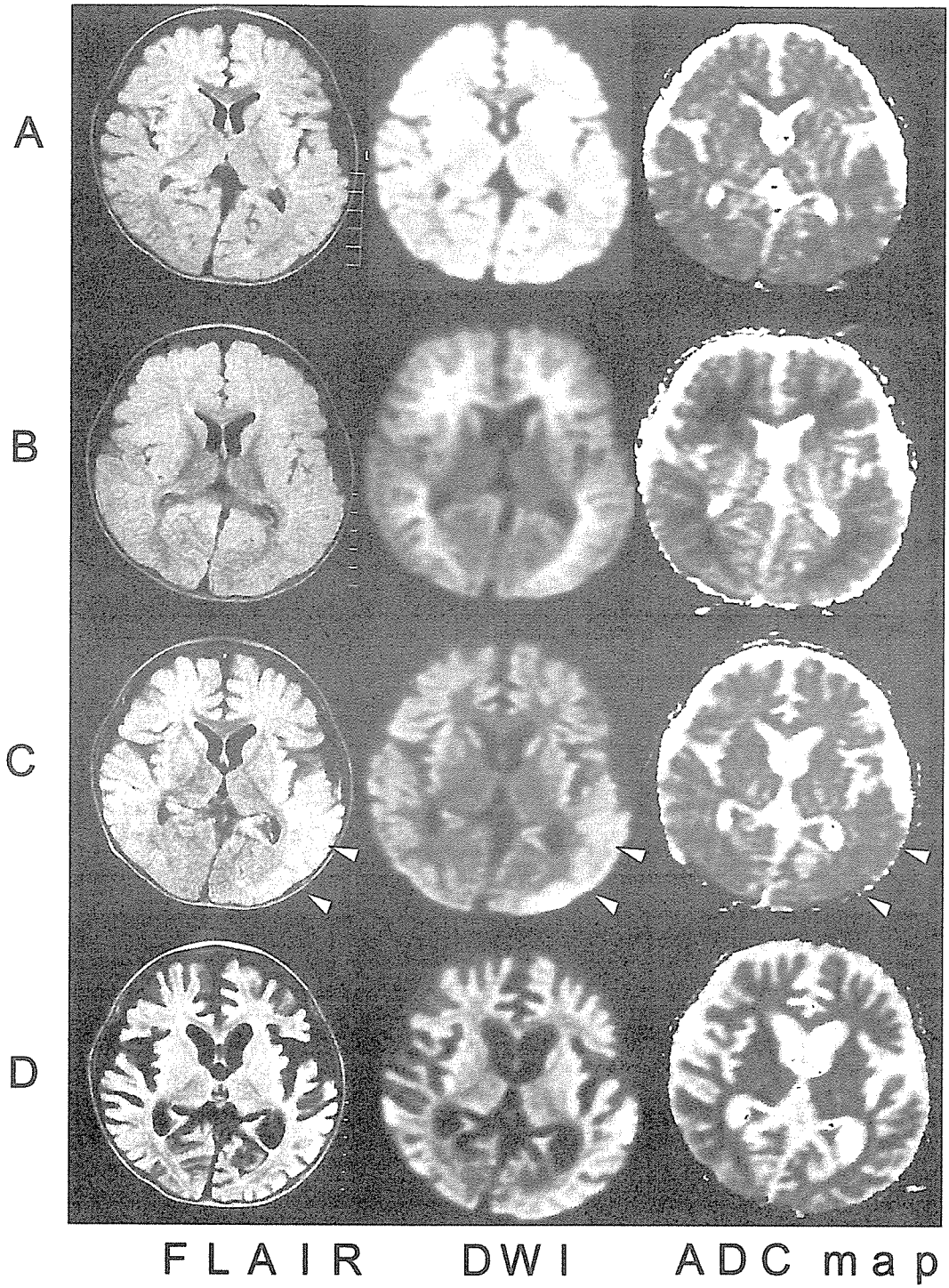

Fig. 2 Fluid-attenuated inversion recovery (FLAIR) images, diffusion-weighted images (DWI), and apparent diffusion coefficient (ADC) maps of Patient 2 at the hyperacute (**A**), acute (**B**), subacute (**C**), and chronic stages (**D**) following status epilepticus. (**A**) Neither brain swelling nor abnormal signal intensity is found in the hyperacute stage. (**B**) Cerebral white matter shows symmetrical hyperintensities on DWI and hypointensities on ADC map in the acute stage. (**C**) White matter hyperintensities disappeared on DWI in the subacute stage. The left temporo-occipital region shows mild hyperintensity on FLAIR image and DWI (arrowhead). The ADC map shows no abnormal signals in the corresponding areas. (**D**) Diffuse brain atrophy progressed in the chronic stage.

Patient 4

Hyperacute stage: CT (days 1 and 3) showed no abnormal findings.

Acute stage (Fig. **4A**): CT (days 5 and 6) demonstrated loss of gray-white junction in the cerebrum. DWI (day 6) revealed symmetrical hyperintensities in the centrum semiovale, whereas no definite abnormalities were detected on T_2WI and FLAIR images. The ADC map showed restricted diffusion in the centrum semiovale.

Subacute stage: Enlargement of the lateral ventricle and widening of the cortical sulci, suggesting diffuse brain atrophy was present on CT (day 15).

Chronic stage (Fig. **4B**): The 2-month follow-up MRI showed disappearance of white matter abnormalities and progression of brain atrophy with diffuse widening of cortical sulci.

CSF cytokines (Table 2)

IL-6 or TNF-α was elevated in each patient. IL-6 was elevated in all patients and TNF-α was elevated in Patients 1 and 2.

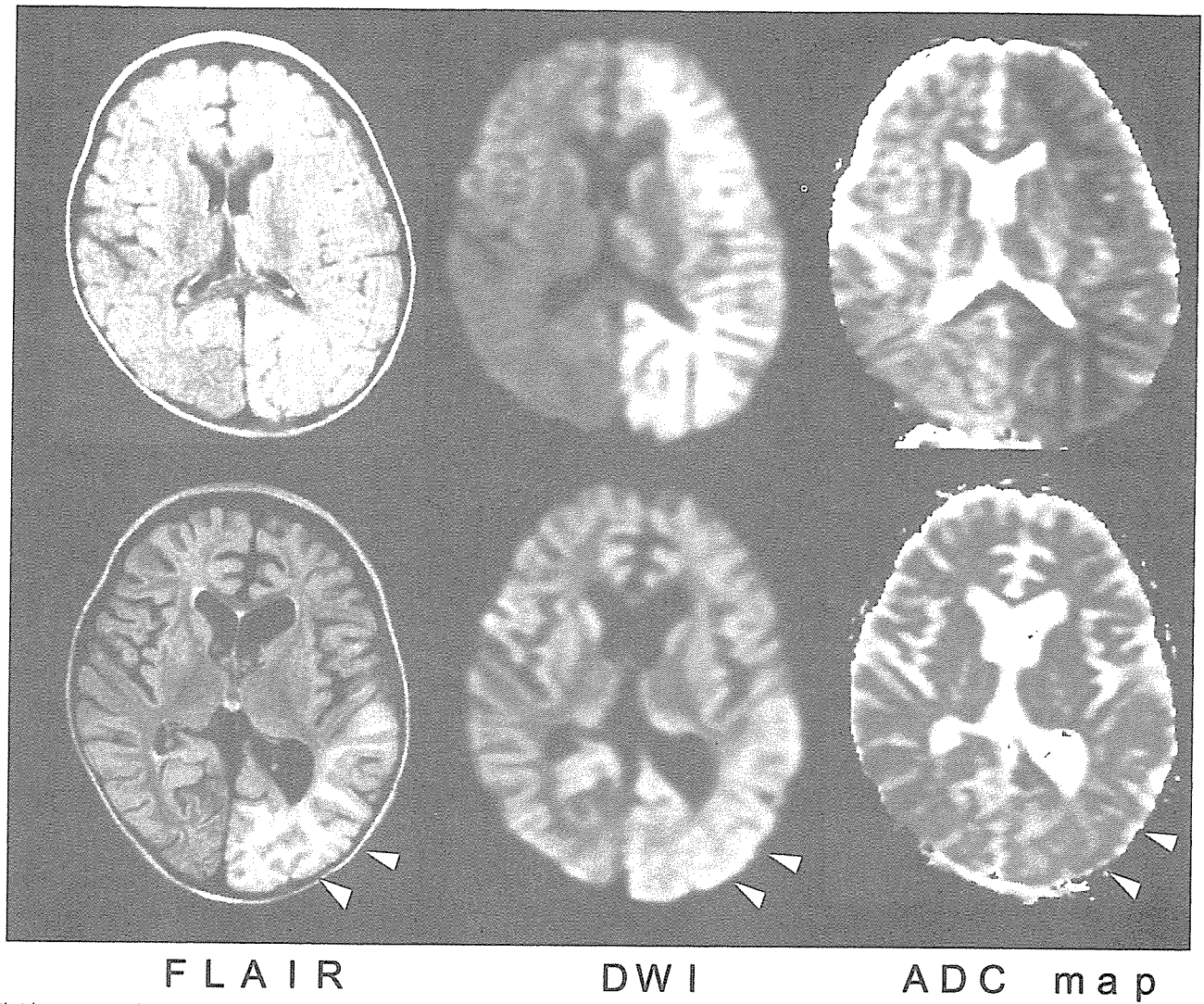

Fig. 3 Fluid-attenuated inversion recovery (FLAIR) images, diffusion-weighted images (DWI), and apparent diffusion coefficient (ADC) maps of Patient 3 at the acute (**A**) and subacute stages (**B**) following status epilepticus. (**A**) Cerebral white matter of the left hemisphere shows hyperintensities on DWI and hypointensities on ADC map in the acute stage. (**B**) MR images show moderate diffuse brain atrophy and residual hyperintensities in the white matter of the left temporal, parietal, and occipital lobes on the FLAIR image and DWI (arrowhead). The ADC map also shows hyperintensities in the corresponding areas (arrowhead).

Other children who had no neurological sequelae after status epilepticus

Seizure duration ranged from 30 to 180 minutes (mean: 52.0, standard deviation: 21.8). In patients with febrile convulsion, seizure duration ranged from 30 to 60 minutes (mean: 42.4, standard deviation: 13.1): seizure duration was significantly longer in the four patients with neurological sequelae than in patients without neurological sequelae ($p = 0.002$, Wilcoxon test). None of the children showed neurological exacerbation or seizure recurrence several days after initial status epilepticus.

Discussion

The most striking neuroimaging findings observed early after status epilepticus in the present patients were hyperintensity on DWI and hypointensity on ADC maps in the white matter. In most previously reported cases, DWI hyperintensity and ADC hypointensity were located dominantly in the restricted gray matter during or early after status epilepticus [4,6,12,14,15 27]. White matter abnormalities on DWI were reported in a few cases [1,7,9,13,14]. Because we experienced four patients who had neurological sequelae out of 42 children with status epilepticus in our hospitals and they all showed pronounced white matter abnormalities on MRI, preferential white matter abnormalities after seizures may not be rare. DWI and ADC maps clearly demonstrated white matter abnormalities while other conventional imaging techniques including FLAIR images failed to detect these findings. As evaluation by DWI and ADC maps has not been routinely performed until a few years ago in Japan, white matter abnormalities could have previously been missed. Moreover, the DWI and ADC abnormalities were only recognized in the restricted periods following status epilepticus (from four to ten days after onset). Hence, white matter abnormalities would be common findings soon after status epilepticus, when cerebral damage permanently occurs.

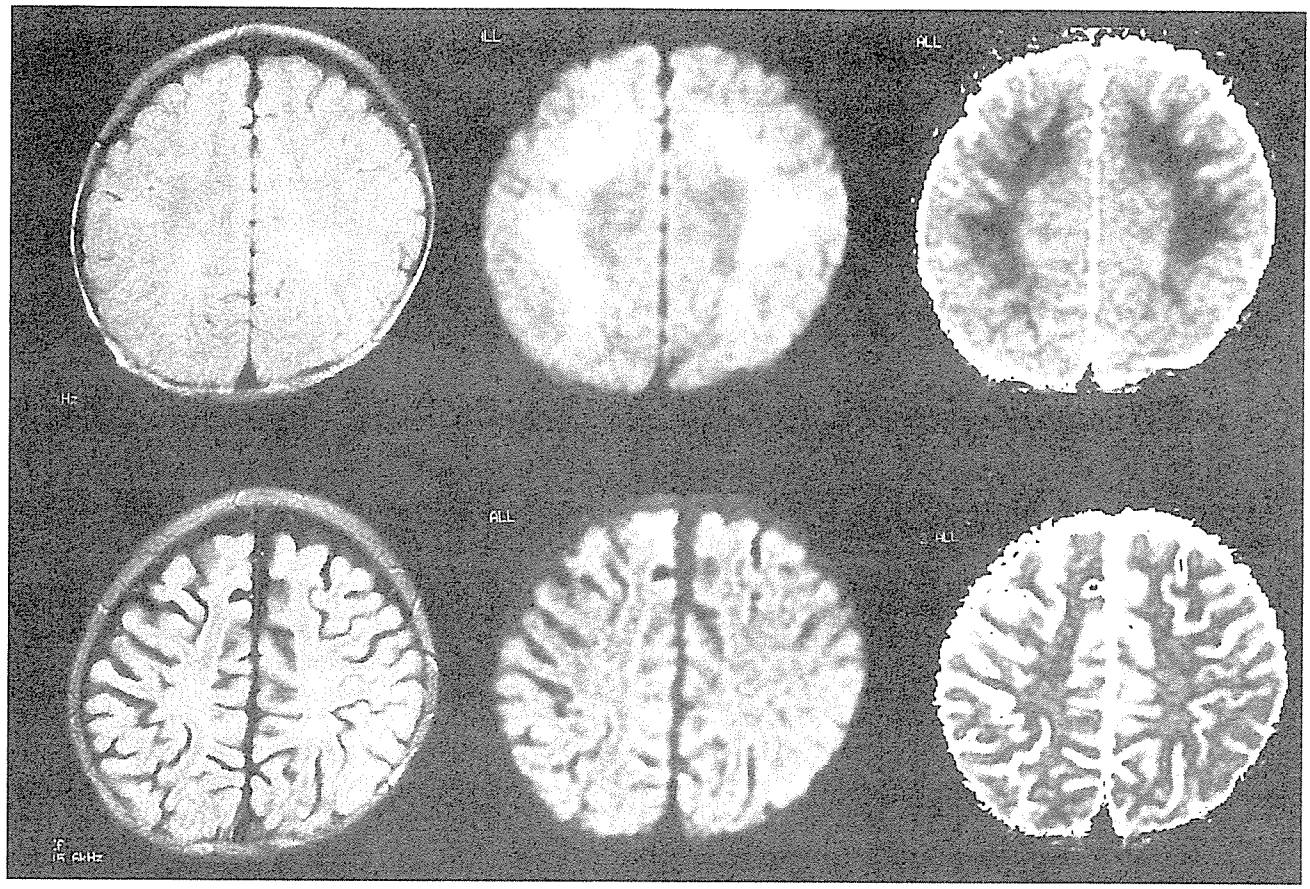

Fig. 4 Fluid-attenuated inversion recovery (FLAIR) images, diffusion-weighted images (DWI), and apparent diffusion coefficient (ADC) maps of Patient 4 at the acute (**A**) and chronic stages (**B**) following status epilepticus. (**A**) DWI shows symmetrical hyperintensities in the subcortical white matter and centrum semiovale in the acute stage. The ADC map shows hypointensities in the corresponding region. (**B**) White matter hyperintensities disappeared on DWI and diffuse brain atrophy progressed in the chronic stage.

The preferential white matter involvement on MRI similar to the present patients has been reported in anoxic-ischemic encephalopathy [2]. Chalela et al. reported seven cases with prominent white matter abnormalities seen on DWI within 7 days after anoxic-ischemic events. High DWI and low ADC were symmetrically and diffusely found in the white matter. In the rat model, oligodendrocyte and astrocyte injury preceded neural injury following ischemia [22]. Medelcu et al. reported biphasic edema after hypoxic-ischemic injury in neonatal rats [21]. The early edema reflected neuronal death and the second edema was associated with glial damage. Severe hypoxemia which directly induced cerebral injury was not present in our patients, indicating that white matter injury can also occur early after status epilepticus. In the pathological study of the human brain of influenza encephalopathy, clinically characterized by prolonged seizure and consciousness disturbance followed by significant brain edema. Nakai et al. found that microglial activation was observed in the gray and white matter and astroglial activation was seen in the white matter [20]. The elevated CSF cytokine levels found in the present patients indicate an activation of glial function. In the rat brain, glial activation and swelling were shown early after status epilepticus [5,23,24]. Glial fibrillary acidic protein levels were elevated in the CSF from patients with status epilepticus [8]. Therefore, prolonged seizure activity can induce glial activation similar to global hypoxia. Glial hyperfunction or hypofunction may lead to the induction of proinflammatory cytokines or nitric oxide, release of excitatory amino acids, or blood-brain barrier breakdown, resulting in both glial and neural injury.

Another possibility for the white matter diffusion abnormality is acute axonal injury due to diffuse cortical damage [18,26]. Watanabe et al. studied axonal function in patients with brain death using anisotropic DWI [26]. They reported that diffusion anisotropy started to decrease 1 to 12 hours and reached isotropy 24 to 44 hours after the onset of brain death. Therefore, restricted diffusion in the white matter may reflect delayed axonal dysfunction secondary to diffuse cortical injury.

One might expect that the white matter abnormalities seen in the acute stage were caused by second seizures four to five days after onset. But this is unlikely, because CT and MRI abnormalities preceded seizure recurrence in Patients 3 and 4. White matter abnormalities could primarily be a consequence of the first status epilepticus. Such delayed imaging findings following status epilepticus were reported in a few cases without seizure recurrence [9,19]. Nevertheless, seizure recurrence might affect further cerebral injury.

Table 2 Clinical characteristics, CSF findings, and prognosis

	Age (months) /sex	Prior neurological disorder	Initial seizure duration (min)	Second seizure		CSF (days of collection)			Prognosis
				Days of onset	Duration (h)	Cell[a]/Protein[b]/Sugar[c]	IL-6[d]	TNF-α[d]	
Patient 1	19/M	Chiari II malformation hydrocephalus, mild developmental delay	180 (lasting)	5	26 (repetitive)	0/3.1/86 (1), 1/1.4/79 (4)	2.3 (1), 10.8 (4)	68.4 (1), 56.6 (4)	severe MR
Patient 2	13/M	none	150 (lasting)	4	1 (lasting)	0/23/134 (1)	12.5 (1)	1041.8 (1)	severe MR
Patient 3	18/F	none	90 (lasting)	5	50 (repetitive)	0/20/130 (1)	NE	NE	severe MR, right hemiparesis
Patient 4	12/M	none	150 (lasting)	5	24 (repetitive)	16/15.4/190 (1)	70.9 (1)	ND (1)	moderate MR

[a]/mm³; [b]mg/dL; [c]mg/dL; [d]pg/mL; F = female; M = male; MR = mental retardation; ND = not detectable; NE = not examined; h = hour; min = minutes

In the subacute and chronic stages, the DWI hyperintensity seen in the white matter at the acute stage resolved, and ADC hypointensity became isointense and then hyperintense. At the same time, T_2 and FLAIR hyperintensity became apparent in both white and gray matter, and diffuse brain atrophy progressed. These signal changes possibly reflect cell damage and gliosis. At the subacute stage in Patient 1, DWI hyperintensity and ADC hypointensity were seen in the occipital cortex, while they were isointense in the hyperacute and acute stages. This highly delayed cytotoxic edema is peculiar and may be secondary to white matter injury.

The clinical course early after status epilepticus has not been well described previously. Other than the present patients, a detailed clinical course was described in a few patients with hemiconvulsion-hemiplegia syndrome [9,13,19]. Their clinical course and imaging findings were quite similar: initial seizures were prolonged and neurological findings were exacerbated along with seizure recurrence several days later. MRI abnormalities were evident at the time of neurological exacerbation. The present patients also showed a biphasic clinical course. Other children in the present study who had no neurological sequelae after status epilepticus showed no biphasic clinical course. Therefore, a biphasic clinical course may be a specific feature and could be a hallmark for neurological sequelae.

The prognosis of status epilepticus varies widely in each patient. We cannot explain why cerebral damage occurs in some but not all patients after status epilepticus. In the present study, patients who had neurological sequelae were all febrile and their initial seizures were significantly prolonged. Pyrexia and seizure duration would be important factors for status epilepticus-associated cerebral injury [16].

To identify the pathophysiology of status epilepticus-associated cerebral injury and protect against cerebral damage, a prospective and systemic study that includes serial imaging and an analysis of CSF cytokines and other cytotoxic substances is essential.

References

1 Akasaka M, Sasaki M, Ehara S, Kamei A, Chida S. Transient decrease in cerebral white matter diffusivity on MR imaging in human herpes virus-6 encephalopathy. Brain Dev 2005; 27: 30–33

2 Chalela JA, Wolf RL, Maldjian JA, Kasner SE. MRI identification of early white matter injury in anoxic-ischemic encephalopathy. Neurology 2001; 56: 481–485

3 Chu K, Kang D-W, Kim J-Y, Chang K-H, Lee SK. Diffusion-weighted magnetic resonance imaging in nonconvulsive status epilepticus. Arch Neurol 2001; 58: 993–998

4 Diehl B, Najm I, Ruggieri P, Foldvary N, Mohamed A, Tkach J et al. Periictal diffusion-weighted imaging in a case of lesional epilepsy. Epilepsia 1999; 40: 1667–1671

5 Evans M, Griffiths T, Meldrum B. Early changes in the rat hippocampus following seizures induced by bicuculline or L-allylglycine: a light and electron microscope study. Neuropathol Appl Neurobiol 1983; 9: 39–52

6 Flacke S, Wüllner U, Keller E, Hamzei F, Urbach H. Reversible changes in echo planar perfusion- and diffusion-weighted MRI in status epilepticus. Neuroradiology 2000; 42: 92–95

7 Freeman JL, Coleman LT, Smith LJ, Shield LK. Hemiconvulsion-hemiplegia-epilepsy syndrome: characteristic early magnetic resonance imaging findings. J Child Neurol 2002; 17: 10–16

8 Gurnett CA, Landt M, Wong M. Analysis of cerebrospinal fluid glial fibrillary acidic protein after seizures in children. Epilepsia 2003; 44: 1455–1458

9 Hisano T, Ohno M, Egawa T, Takano T, Shimada M. Changes in diffusion-weighted MRI after status epilepticus. Pediatr Neurol 2000; 22: 327–329

10 Hong K-S, Cho Y-J, Lee SK, Jeong S-W, Kim WK, Oh EJ. Diffusion changes suggesting predominant vasogenic oedema during partial status epilepticus. Seizure 2004; 13: 317–321

11 Ichiyama T, Morishima T, Isumi H, Matsufuji H, Matsubara T, Furukawa S. Analysis of cytokine levels and NF-κB activation in peripheral blood mononuclear cells in influenza virus-associated encephalopathy. Cytokine 2004; 27: 31–37

12 Kassem-Moussa H, Provenzale JM, Petrella JR, Lewis DV. Early diffusion-weighted MR imaging abnormalities in sustained seizure activity. AJR Am J Roentgenol 2000; 174: 1304–1306

[13] Kawada J, Kimura H, Yoshikawa T, Ihira M, Okumura A, Morishima T et al. Hemiconvulsion-hemiplegia syndrome and primary human herpes virus 7 infection. Brain Dev 2004; 26: 412 – 414
[14] Kim J-A, Chung JI, Yoon PH, Kim DI, Chung T-S, Kim E-J et al. Transient MR signal changes in patients with generalized seizure or status epilepticus: periictal diffusion-weighted imaging. AJNR 2001; 22: 1149 – 1160
[15] Lansberg MG, O'Brien MW, Norbash AM, Moseley ME, Morrell M, Albers GW. MRI abnormalities associated with partial status epilepticus. Neurology 1999; 52: 1021 – 1027
[16] Maegaki Y, Kurozawa Y, Hanaki K, Ohno K. Risk factors for fatality and neurological sequelae after status epilepticus in children. Neuropediatrics 2005; 36; 186 – 192
[17] Maytal J, Shinnar S, Moshé SL, Alvarez LA. Low morbidity and mortality of status epilepticus in children. Pediatrics 1989; 83: 323 – 331
[18] Mazumdar A, Mukherjee P, Miller JH, Malde H, McKinstry RC. Diffusion-weighted imaging of acute corticospinal tract injury preceding Wallerian degeneration in the maturing human brain. AJNR 2003; 24: 1057 – 1066
[19] Morimoto T, Fukuda M, Suzuki Y, Kusu M, Kida K. Sequential changes of brain CT and MRI after febrile status epilepticus in a 6-year-old girl. Brain Dev 2002; 24: 190 – 193
[20] Nakai Y, Itoh M, Mizuguchi M, Ozawa H, Okazaki E, Kobayashi Y et al. Apoptosis and microglial activation in influenza encephalopathy. Acta Neuropathol 2003; 105: 233 – 239
[21] Nedelcu J, Klein MA, Aguzzi A, Boesiger P, Martin E. Biphasic edema after hypoxic-ischemic brain injury in neonatal rats reflects early neuronal and late glial damage. Pediatr Res 1999; 46: 297 – 304
[22] Pantoni L, Garcia JH, Gutierrez JA. Cerebral white matter is highly vulnerable to ischemia. Stroke 1996; 27: 1641 – 1647
[23] Rizzi M, Perego C, Aliprandi M, Richichi C, Ravizza T, Colella D et al. Glia activation and cytokine increase in rat hippocampus by kainic acid-induced status epilepticus during postnatal development. Neurobiol Dis 2003; 14: 494 – 503
[24] Schmidt-Kastner R, Ingvar M. Loss of immunoreactivity for glial fibrillary acidic protein (GFAP) in astrocytes as a marker for profound tissue damage in substantia nigra and basal cortical areas after status epilepticus induced by pilocarpine in rat. Glia 1994; 12: 165 – 172
[25] Verity CM, Ross EM, Golding J. Outcome of childhood status epilepticus and lengthy febrile convulsions: findings of national cohort study. BMJ 1993; 307: 225 – 228
[26] Watanabe T, Honda Y, Fujii Y, Koyama M, Tanaka R. Serial evaluation of axonal function in patients with brain death by using anisotropic diffusion-weighted magnetic resonance imaging. J Neurosurg 2004; 100: 56 – 60
[27] Wieshmann UC, Symms MR, Shorvon SD. Diffusion changes in status epilepticus. Lancet 1997; 350: 493 – 494

available at www.sciencedirect.com

SCIENCE DIRECT®

www.elsevier.com/locate/brainres

ELSEVIER

BRAIN RESEARCH

Research Report

Altered glycosylation of α-dystroglycan in neurons of Fukuyama congenital muscular dystrophy brains

Yoshiaki Saito[a,b,*], *Tomoko Yamamoto*[c], *Masashi Mizuguchi*[d], *Makio Kobayashi*[c], *Kayoko Saito*[a], *Kousaku Ohno*[b], *Makiko Osawa*[a]

[a]*Department of Pediatrics, Tokyo Women's Medical University, Japan*
[b]*Division of Child Neurology, Institute for Neurological Sciences, Tottori University, Japan*
[c]*Department of Pathology, Tokyo Women's Medical University, Japan*
[d]*Department of Pediatrics, Tokyo University, Japan*

ARTICLE INFO

Article history:
Accepted 27 December 2005
Available online 7 February 2006

Keywords:
α-Dystroglycan
Fukutin
Fukuyama congenital muscular dystrophy
Glycosylation
Glia-limitans

Abbreviations:
FCMD, Fukuyama congenital muscular dystrophy
α-DG, α-dystroglycan

ABSTRACT

To test the hypothesis that the disruption of fukutin protein produces the brain pathology through hypoglycosylation of α-dystroglycan (α-DG), we immunostained Fukuyama congenital muscular dystrophy (FCMD) brains with an antibody that recognizes the polysaccharide epitope of α-DG. Immunoreactivity of the glia-limitans along the cortical surface, as well as that of the glial endfeet around vessel walls, was preserved in the FCMD cerebrum. However, fragmentation of the immunostained glia-limitans was noted in association with parenchymal protrusion and gyral fusion. In the FCMD cerebellum, this fragmentation of α-DG labeling was limited to the area of micropolygyria, and immunostaining at the glia-limitans and vessel walls was comparable to that of the control brains, in structurally normal areas. In the hippocampus, neurons of the dentate gyrus and corpus ammonis were immunopositive for α-DG in control subjects, but this staining was markedly decreased in FCMD brains. In contrast, immunolabeling of blood vessels and the glia-limitans was preserved in this region. Fukutin antisera clearly labeled hippocampal neurons in control brains, while this labeling was decreased in FCMD brains. Thus, hypoglycosylation of α-DG was evident in neurons, but not in the glial cell population of FCMD brains. This suggests that the mechanism of α-DG glycosylation may differ between neurons and glial cells, and that a fukutin gene defect may result in functional disruption through hypoglycosylation of both neuronal and glial α-DG.

* *Corresponding author.* Division of Child Neurology, Institute for Neurological Sciences, Tottori University, 36-1 Nishi-cho, Yonago 683-8504, Japan. Fax: +81 859 38 6779.
E-mail address: saitoyo@grape.med.tottori-u.ac.jp (Y. Saito).

0006-8993/$ – see front matter © 2006 Elsevier B.V. All rights reserved.
doi:10.1016/j.brainres.2005.12.108

1. Introduction

Fukuyama congenital muscular dystrophy (FCMD) is caused by mutations in the fukutin gene (Kobayashi et al., 1998), the product of which is involved in the glycosylation of α-dystroglycan (α-DG) (Aravind and Koonin, 1999; Michele et al., 2002), a central component of the dystrophin–glycoprotein complex (Ervasti and Campbell, 1993; Henry and Campbell, 1999; Ibraghimov-Beskrovnaya et al., 1992). Hypoglycosylation of α-DG results in the decreased binding of laminin at the sarcolemma and in the subsequent dystrophic pathology of skeletal muscles (Michele et al., 2002).

As for the central nervous system, FCMD brains are characterized by cerebral and cerebellar micropolygyria (Kamoshita et al., 1976). Based on the breached glia-limitans and the protrusion of glial–neuronal tissue into the subarachnoid space, a fragile glia-limitans has been hypothesized to be a cardinal feature of the pathological process in FCMD brains (Nakano et al., 1996; Takada et al., 1987). The presence of α-DG in the glia-limitans, and in the glial endfeet of vessel walls (Michele et al., 2002; Zaccaria et al., 2001), supports the hypothesis that hypoglycosylation of α-DG results in decreased binding of glial α-DG with extracellular matrix proteins. Decreased integrity of the glia-limitans may be responsible for the protrusion of brain parenchyma and overmigration of neurons beyond the pial surface during cerebral corticogenesis. However, in contrast to the findings in muscle tissue, hypoglycosylation of α-DG has not been identified in the glia-limitans of FCMD brains. In addition, fukutin protein has been localized in both neurons and glial cells (Ohtsuka-Tsurumi et al., 2004; Saito et al., 2000; Sasaki et al., 2000; Yamamoto et al., 2002). In this study, we immunostained FCMD brains with an antibody that recognizes the polysaccharide epitope of α-DG. Interestingly, the immunoreactivity of glycosylated α-DG in the subpial glia-limitans was not ubiquitously disrupted. On the other hand, hypoglycosylation of α-DG was suggested in hippocampal neurons of FCMD brains. This differential hypoglycosylation may provide a clue to understanding the pathological process in FCMD brains.

2. Results

The α-DG antibody labeled the glia-limitans at the cortical surface and the vessel walls in the control cerebrum (Fig. 1A) and cerebellum (Fig. 1D). In FCMD brains, the continuity of glia-limitans staining was occasionally interrupted at regions with parenchymal protrusions beyond the pial surface (Fig. 1B). Fragmentation of α-DG immunopositive membrane was also noted at the gyral fusion (Fig. 1C). In the FCMD cerebellum, immunostaining at the glia-limitans and vessel walls was comparable to that in the control brains, in areas without micropolygyria (Fig. 1E). The fragmentation of α-DG labeling at the glia-limitans was restricted to the area of micropolygyria (Fig. 1F). Laminin immunolabeling was fragmented and correlated with that of α-DG in the structurally disordered regions of FCMD cerebrum and cerebellum (Figs. 2A and B). α-DG immunolabeling on capillary walls was confirmed by double staining with antifactor VIII (Figs. 2C to E). In the hippocampus, neurons of the dentate gyrus and the corpus ammonis were immunopositive for α-DG in control subjects (Figs. 3A and C), but this staining was markedly decreased in all of the FCMD brains (Figs. 3B and D). In contrast, immunolabeling of blood vessels and the glia-limitans was preserved in this region. The immunolabeling disappeared completely in negative control experiments (not shown). Other than the hippocampus, α-DG immunolabeling was not detected in the cerebral and cerebellar neurons of either control or FCMD brains.

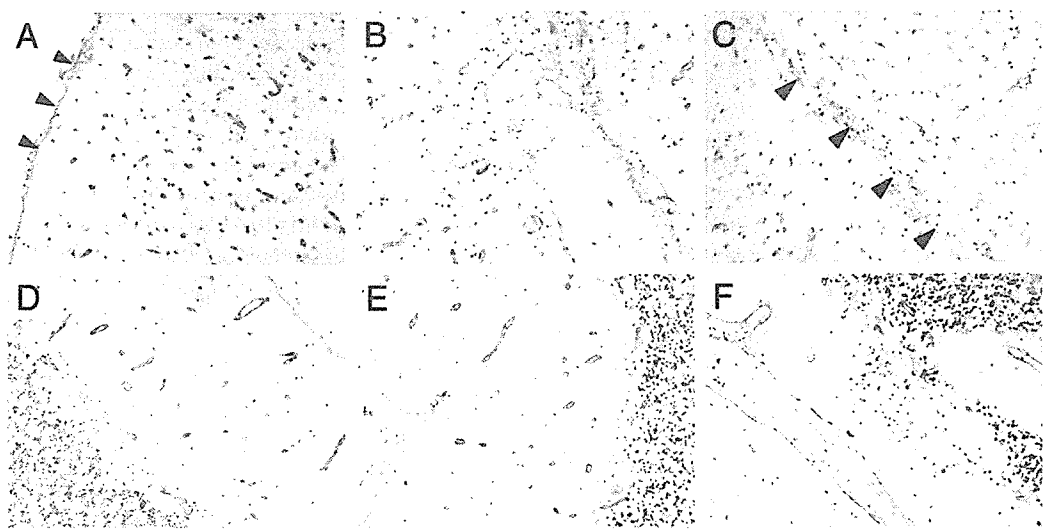

Fig. 1 – α-dystroglycan (α-DG) immunoreactivity in control (A and D) and FCMD (B, C, E, and F) brains. The α-DG positive glia-limitans is continuous in the control cerebrum (arrowheads in A), but fragmentary on the cortical surface (B) and at the cortical fusion (C, arrowheads) in FCMD brains. The continuity of the α-DG positive glia-limitans is preserved in the control cerebellum (D) and in the FCMD cerebellum in areas with normal structure (E), but is disrupted in the FCMD cerebellum in areas of micropolygyria (F). A to F: 200×.

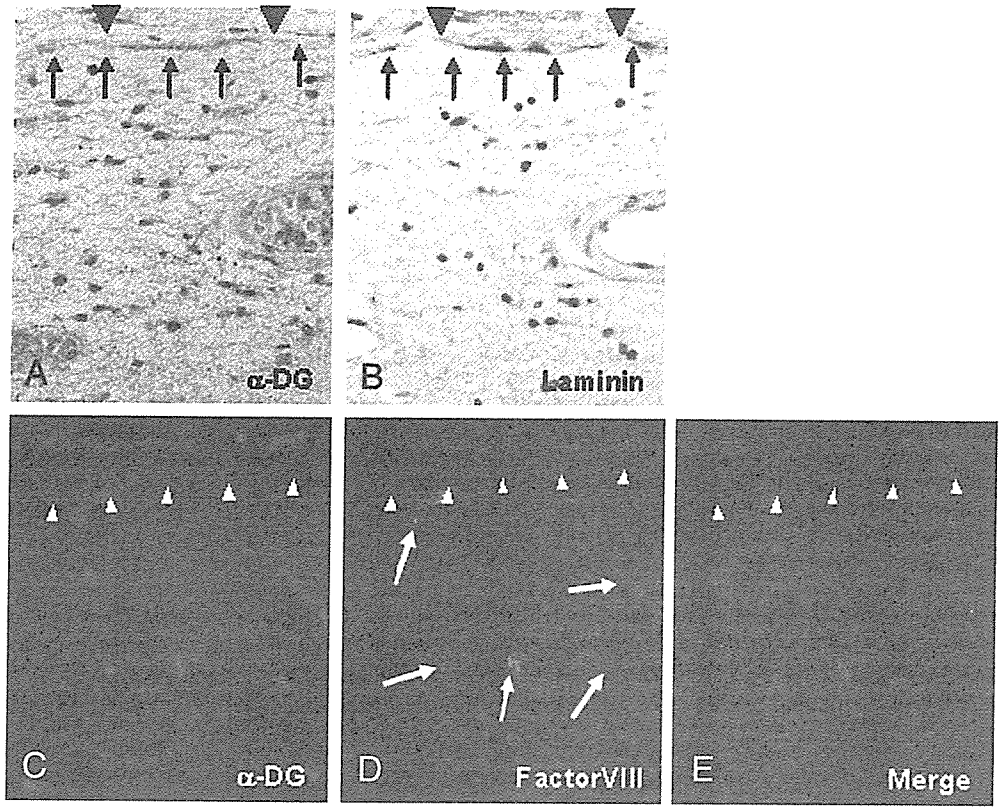

Fig. 2 – (A and B) Immunolabeling of glia-limitans (arrows) with α-DG (A) and laminin (B) is decreased at comparable sites (A and B) in consecutive sections of an FCMD cerebrum. (C–E) α-DG (C) is co-localized with factor VIII (D) at capillary walls. Arrowheads: glia-limitans, arrows: capillaries. A to E: 400×.

The fukutin antisera labeled the neurons of the corpus ammonis (Fig. 4B), and this labeling was decreased in the FCMD brains (Fig. 4C). The labeling of dentate gyrus neurons was weak in control subjects (Fig. 4E) and FCMD patients (Fig. 4F), making the difference between these groups less evident than in the corpus ammonis. Other than this hippocampal expression, immunolabeling was not detected in the cerebral and cerebellar neurons of either control or FCMD brains. No

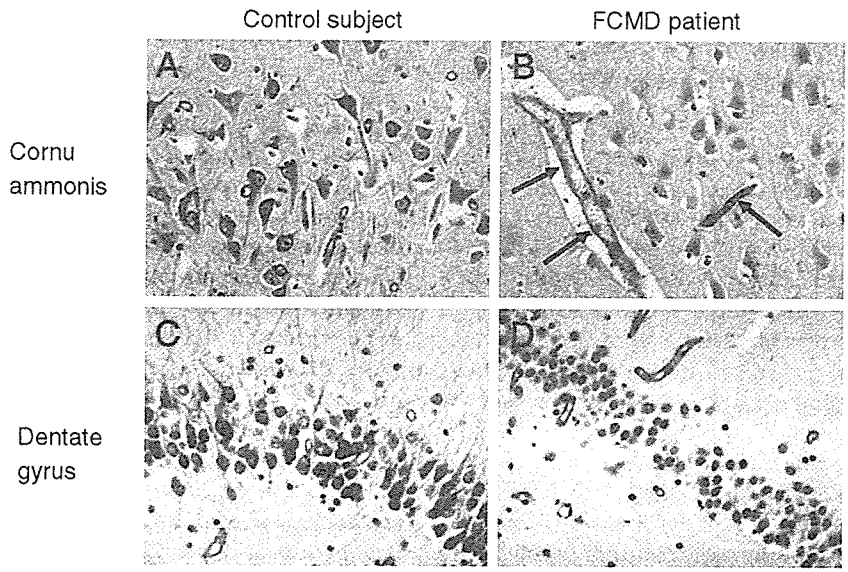

Fig. 3 – α-dystroglycan (α-DG) immunoreactivity in the hippocampus. Neurons in the cornu ammonis 2 area (A) and dentate gyrus (C) are immunopositive for α-DG in control brains, but are immunonegative in FCMD brains (B and D). Note that vessel walls are immunopositive for α-DG in FCMD brains (arrows in panel B). A to D: 400×.

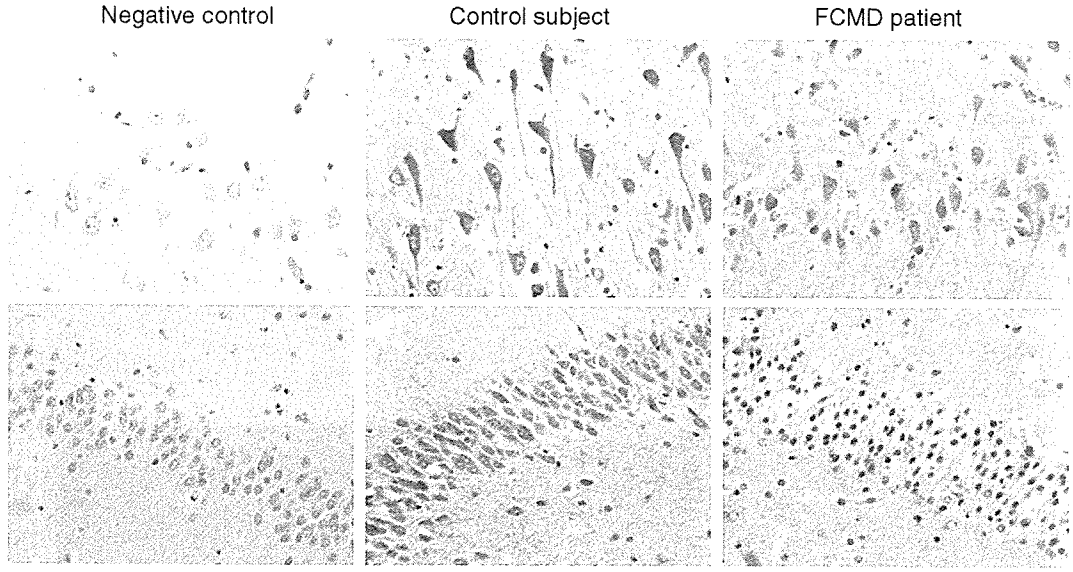

Fig. 4 – Hippocampal fukutin immunoreactivity in control (A, B, D, and E) and FCMD (C and F) brains, stained with the anti-C1 (B, C, E, and F) antiserum. Primary antibody was replaced with preabsorbed antiserum in negative control experiments (A and D). Labeling is intense in neurons of the cornu ammonis in control brains (A), but is diminished in FCMD brains (C). The labeling is weak in the dentate gyrus, and the difference between the control (E) and FCMD (F) is less evident. A to H: 400×.

immunoproducts were seen on slides incubated with the preimmune sera (Figs. 4A and D). The data are summarized in Fig. 5.

3. Discussion

The data presented here suggest co-expression of α-DG and fukutin in the hippocampal neurons of humans. Decreased labeling of α-DG with VIA4-1 in this cell population in FCMD brains supports the involvement of fukutin in the glycosylation process of α-DG, as is the case in skeletal muscle (Hayashi et al., 2001; Michele et al., 2002).

In recent years, α-DG expression in the glia-limitans has been highlighted, since it strongly supports the hypothesis

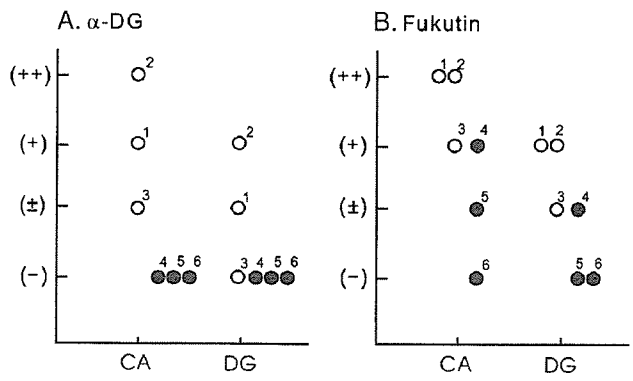

Fig. 5 – Summary of the immunohistochemical findings. Open circle: control subject, filled circle: FCMD patient. (−): negative, (±): weakly positive, (+): moderately positive, (++): intensely positive. CA: cornu ammonis, DG: dentate gyrus. 1 to 3: control subjects, 4 to 6: FCMD patients.

that the fragile glia-limitans is essential to the pathogenesis of micropolygyria. However, there has been controversy regarding the expression pattern of α-DG in the central nervous system. α-DG has been localized to glial cells (Michele et al., 2002; Moore et al., 2002), neurons (Górecki et al., 1994), or both (Zaccaria et al., 2001), in mammalian brains by means of in situ hybridization (Górecki et al., 1994) and immunohistochemistry (Michele et al., 2002; Moore et al., 2002; Zaccaria et al., 2001). Differences in affinity among antibodies may account for this discrepancy, or the antigenicity of α-DG itself may differ between neurons and glial cells, as discussed below. In any case, neuronal expression of α-DG in the hippocampus has been commonly described in several previous reports (Górecki et al., 1994; Zaccaria et al., 2001), and is consistent with the present observations. Decreased immunolabeling of α-DG in hippocampal neurons is compatible with blunted long-term hippocampal potentiation in the brain-selective α-DG knockout mouse (Moore et al., 2002). Since α-DG may participate in synaptic function through clustering of the dystrophin-glycoprotein complex with GABA receptors (Knuesel et al., 2001; Levi et al., 2002; Litov et al., 1990), hypoglycosylation of neuronal α-DG may account for the epileptic seizures and intellectual disabilities of FCMD patients.

Fragmentation of α-DG immunostaining with VIA4-1 antibody correlated with that of laminin immunostaining of glia-limitans at sites of micropolygyria and subarachnoid parenchymal protrusion in FCMD brains. This was compatible with preceding studies using electron microscopy, which showed breaches of the glia-limitans that were penetrated by glial–neuronal tissue (Nakano et al., 1996). On the other hand, unexpectedly, α-DG immunoreactivity with this antibody was preserved in the glia-limitans where the integrity of the cortical structure was preserved, or in the fragmented glia-limitans itself, as well as in vessel walls. This was in

contrast to the reduction of staining in FCMD skeletal muscle with the same antibody (Hayashi et al., 2001). The moiety of the α-DG polysaccharide chain differs between muscle and other tissues. α-DG is identified as a 120-kDa band in brain homogenates, in contrast to the 156-kDa band in skeletal muscle (Campbell and Kahl, 1989; Gee et al., 1993; Herrmann et al., 2000). Hypoglycosylation of α-DG has been identified in FCMD muscles, by demonstrating the absence of monoclonal antibody-reactive α-DG, and the reduction in molecular weight of the core antibody-reactive α-DG (Michele et al., 2002). The former antibodies, including VIA4-1, recognize the polysaccharide epitope, and the latter binds to the polypeptide backbone of α-DG. Hayashi et al. (2001) reported that VIA4-1-reactive α-DG with a normal molecular weight was present but at a reduced level in FCMD brains. Consistent with our present data, they observed the intact staining of blood vessels with this antibody in the FCMD cerebellum. Interestingly, the VIA4-1-reactive punctate labeling of Purkinje cells was reduced in the FCMD brain, in contrast to the normal labeling pattern with a possible core antibody. Taken together, these findings indicate that the α-DG in vascular glial endfeet is normally glycosylated, while the glycosylation of α-DG in neurons is disordered, in FCMD brains. Accordingly, we hypothesize that the glycosylation status of α-DG may differ between neurons and glial cells under physiological conditions. Differential roles of α-DG glycosylation enzymes in individual organs, as identified in the kidney (Grewal et al., 2005), may be extended to this intra-organ differentiation. The VIA4-1 antibody, originally raised against muscle-type α-DG (Ervasti et al., 1990), may have a higher affinity for the polysaccharide epitope of glial cells than for that of neurons. Thus, it is even possible that fukutin and other glycoyslation enzymes (De Bernabé et al., 2002; Grewal et al., 2001; Michele and Campbell, 2003; Yoshida et al., 2001) may have different roles for the glycosylation of neuronal and glial α-DG. This assumption may provide a plausible explanation for the discrepancy between the labeling pattern of the monoclonal and polyclonal α-DG antibodies in brain tissues. Both α-DG and fukutin have been localized to migrating cortical neurons during corticogenesis, but the glycosylation status of α-DG in this population has not been examined in FCMD patients. Further study of this issue is warranted in order to better understand the pathogenesis of morphological and functional abnormalities of FCMD brain.

Although there is a population of immunoreactive α-DG-immunoreactive glial cells in FCMD brain, these cells might be functionally disrupted, via altered glycosylation status and decreased laminin binding affinity. α-DG immunolabeling was further diminished at "breaches" of the glia-limitans, concurrent with loss of laminin immunolabeling. These suggest that laminin binding is disrupted when functional glial α-DG is absent, at sites where the glia-limitans may be particularly fragile. Interestingly, anti-α-DG antibody inhibits migration of cerebellar granule cells, possibly by influencing the attachment of granule neurons to the α-DG-expressing Bergmann glial cells (Qu and Smith, 2004). Disruption of α-DG on glial cells, other than at the glia-limitans, may also be involved in the pathogenesis of micropolygyria in FCMD through a neuronal–glial interaction.

In conclusion, we demonstrated preserved immunolabeling of α-DG polysaccharide chain in glial cells, and a reduction of this labeling in hippocampal neurons, in FCMD brains. Fukutin immunolabeling was also decreased in these neurons. These observations suggest that a fukutin protein defect may result in hypoglycosylation of neurons. The pathogenesis of morphological and functional abnormalities in the FCMD brain should be explored in terms of the functional role of glycosylated α-DG in neurons of developing and mature brains.

4. Experimental procedures

Tissues from three FCMD patients (13–17 years old, M:F = 2:1) and three control subjects (all 14 years of age) were obtained at autopsy. Analysis of the fukutin gene revealed homozygous 3-kb insertions in all three FCMD patients. For immunohistochemistry, we took samples from the cerebral cortex, hippocampus, and cerebellum, and compared the results of FCMD cases with those of control subjects.

Mouse monoclonal antibody against α-DG (VIA4-1; Upstate Biochemistry, Lake Placid, NY, diluted 1:20) was used for immunohistochemistry. VIA4-1 has been shown to recognize the glycosylated epitope of α-DG, and immunolabeling with this antibody is decreased in FCMD muscles (Hayashi et al., 2001). Polyclonal antisera against human fukutin were raised in rabbits as described previously (Saito et al., 2000). Synthetic amino acid peptides, corresponding to residues 37–49 (N1 antigen) and 448–461 (C1 antigen), were used for immunization. The anti-C1 and anti-N1 antisera were diluted at 1:3000 (anti-N1) and 1:2000 (anti-C1) for immunohistochemistry. To identify the structural glia-limitans and capillaries, we performed double staining and immunostaining on consecutive sections using antibodies to α-DG and laminin (rabbit polyclonal, 1:20, Progen, Heidelberg) or factor VIII (rabbit polyclonal, 1:50, ZYMED, South San Francisco, CA). For negative control experiments, the primary antisera were omitted or replaced with preimmune sera of rabbits (for fukutin).

After deparaffinization, the sections were immersed in 3% hydrogen peroxide in phosphate-buffered saline (PBS) for 5 min to abolish endogenous peroxidase activity. Microwave treatment for 13 min at 95 °C was performed to retrieve the antigens. Nonspecific binding was blocked with 10% horse serum. The sections were then incubated for 48 h at 4 °C with the primary antibody, followed by incubation with biotinylated goat anti-mouse IgG antibody for 1 h and then with preoxidase-conjugated streptavidin–biotin complex (Vecstatin ABC kit, Vector, Burlingame, CA) at room temperature for 30 min. Between steps, the sections were washed thoroughly three times in PBS. The immunoproducts were visualized with 0.05% 3,3′-diaminobenzidine and 0.0085% H_2O_2 in PBS. The specimens were counterstained with hematoxylin. For double staining, Cy3-conjugated anti-rabbit IgG (1:200, Jackson Immunoresearch Laboratory, West Grove, PA) and FITC-conjugated donkey anti-mouse IgG (1:200, Jackson Immunoresearch Laboratory) were used as secondary antibodies and were incubated for 6 h.

REFERENCES

Aravind, L., Koonin, E.V., 1999. The fukutin protein family-predicted enzymes modifying cell-surface molecules. Curr. Biol. 9, R836–R837.

Campbell, K.P., Kahl, S.D., 1989. Association of dystrophin and an integral membrane protein. Nature 338, 259–262.

De Bernabé, D.B.-V., Currier, S., Steinbrecher, A., Celli, J., van Beusekom, E., van der Zwaag, B., Kayserili, H., Merlini, L., Chitayat, D., Dobyns, W.B., Cormand, B., Lehesjoki, A.-E., Cruces, J., Voit, T., Walsh, C.A., van Bokhoven, H., Brunner, H.G., 2002. Mutations in the O-mannosyltransferase gene *POMT1* give rise to the severe neuronal migration disorder Walker–Warburg syndrome. Am. J. Hum. Genet. 71, 1033–1043.

Ervasti, J.M., Campbell, K.P., 1993. A role for the dystrophin–glycoprotein complex as a transmembrane linker between laminin and actin. J. Cell Biol. 122, 809–823.

Ervasti, J.M., Ohlendieck, K., Kahl, S.D., Gaver, M.G., Campbell, K.P., 1990. Deficiency of a glycoprotein component of the dystrophin complex in dystrophic muscle. Nature 345, 315–319.

Gee, S.H., Blacher, R.W., Douville, P.J., Provost, P.R., Yurchenco, P.D., Carbonetto, S., 1993. Laminin-binding protein 120 from brain is closely related to the dystrophin-associated glycoprotein, dystroglycan, and binds with high affinity to the major heparin binding domain of laminin. J. Biol. Chem. 268, 14972–14980.

Górecki, D.C., Derry, J.M.J., Barnard, E.A., 1994. Dystroglycan: brain localization and chromosome mapping in the mouse. Hum. Mol. Genet. 3, 1589–1597.

Grewal, P.K., Holzfeind, P.J., Bittner, R., Hewitt, J.E., 2001. Mutant glycosyltransferase and altered glycosylation of α-dystroglycan in the myodystrophy mouse. Nat. Genet. 28, 151–154.

Grewal, P.K., McLaughlan, J.M., Moore, J.C., Browning, C.A., Hewitt, J.E., 2005 (Jun 15). Characterization of the LARGE family of putative glycosyltransferases associated with dystroglycanopathies. Glycobiology 15, 912–923.

Hayashi, Y.K., Ogawa, M., Tagawa, K., Noguchi, S., Ishihara, T., Nonaka, I., Arahata, K., 2001. Selective deficiency of α-dystroglycan in Fukuyama-type congenital muscular dystrophy. Neurology 57, 115–121.

Henry, M.D., Campbell, K.P., 1999. Dystroglycan inside and out. Curr. Opin. Cell Biol. 11, 602–607.

Herrmann, R., Straub, V., Blank, M., Kutzick, C., Franke, N., Jacob, E.N., Lenard, H.G., Kröger, S., Voit, T., 2000. Dissociation of the dystroglycan complex in caveolin-3-deficient limb girdle muscular dystrophy. Hum. Mol. Genet. 9, 2335–2340.

Ibraghimov-Beskrovnaya, O., Ervasti, J.M., Leveille, J., Slaughter, C.A., Sernett, S.W., Campbell, K.P., 1992. Primary structure of dystrophin-associated glycoproteins linking dystrophin to the extracellular matrix. Nature 355, 696–702.

Kamoshita, S., Konishi, Y., Segawa, M., Fukuyama, Y., 1976. Congenital muscular dystrophy as a disease of the central nervous system. Arch. Neurol. 33, 513–516.

Knuesel, I., Zuellig, R.A., Schaub, M.C., Fritschy, J.-M., 2001. Alterations in dystrophin and utrophin expression parallel the reorganization of GABAergic synapses in a mouse model of temporal lobe epilepsy. Eur. J. Neurosci. 13, 1113–1124.

Kobayashi, K., Nakahori, Y., Miyake, M., Matsumura, K., Kondo-Iida, E., Nomura, Y., Segawa, M., Yoshioka, M., Saito, K., Osawa, M., Hamano, K., Sakakihara, Y., Nonaka, I., Nakagome, Y., Kanazawa, I., Nakamura, Y., Tokunaga, K., Toda, T., 1998. An ancient retrotransposal insertion causes Fukuyama-type congenital muscular dystrophy. Nature 394, 388–392.

Levi, S., Grady, R.M., Henry, M.D., Campbell, K.P., Sanes, J.R., Craig, A.M., 2002. Dystroglycan is selectively associated with inhibitory GABAergic synapses but is dispensable for their differentiation. J. Neurosci. 22, 4274–4285.

Litov, H.G.W., Byers, T.J., Watkins, S.C., Kunkel, L.M., 1990. Localization of dystrophin to postsynaptic regions of central nervous system cortical neurons. Nature 348, 725–728.

Michele, D.E., Campbell, K.P., 2003. Dystrophin-glycoprotein complex: post-translational processing and dystroglycan function. J. Biol. Chem. 278, 15457–15460.

Michele, D.E., Barresi, R., Kanagawa, M., Saito, F., Cohn, R.D., Satz, J.S., Dollar, J., Nishino, I., Kelley, R.I., Somer, H., Straub, V., Mathews, K.D., Moore, S.A., Campbell, K.P., 2002. Post-transcriptional disruption of dystroglycan–ligand interactions in congenital muscular dystrophies. Nature 418, 417–422.

Moore, S.A., Saito, F., Chen, J., Michele, D.E., Henry, M.D., Messing, A., Cohn, R.D., Ross-Barta, S.E., Westra, S., Williamson, R.A., Hoshi, T., Campbell, K.P., 2002. Deletion of brain dystroglycan recapitulates aspects of congenital muscular dystrophy. Nature 418, 422–425.

Nakano, I., Funahashi, M., Takada, K., Toda, T., 1996. Are breaches in the glia limitans the primary cause of the micropolygyria in Fukuyama-type congenital muscular dystrophy (FCMD)? Pathological study of the cerebral cortex of an FCMD fetus. Acta Neuropathol. 91, 313–321.

Ohtsuka-Tsurumi, E., Saito, Y., Yamamoto, T., Voit, T., Kobayashi, M., Osawa, M., 2004. Co-localization of fukutin and alpha-dystroglycan in the mouse central nervous system. Brain Res. Dev. Brain Res. 152, 121–127.

Qu, Q., Smith, F.I., 2004. Alpha-dystroglycan interactions affect cerebellar granule neuron migration. J. Neurosci. Res. 76, 771–782.

Saito, Y., Mizuguchi, M., Oka, A., Takashima, S., 2000. Fukutiin protein is expressed in neurons of the normal developing human brain but is reduced in Fukuyama-type congenital muscular dystrophy brain. Ann. Neurol. 47, 756–764.

Sasaki, J., Ishikawa, K., Kobayashi, K., Kondo-Iida, E., Fukayama, M., Mizusawa, H., Takashima, S., Sakakihara, Y., Nakamura, Y., Toda, T., 2000. Neuronal expression of the fukutin gene. Hum. Mol. Genet. 9, 3083–3090.

Takada, K., Nakamura, H., Suzumori, K., Ishikawa, T., Sugiyama, N., 1987. Cortical dysplasia in a 23-week fetus with Fukuyama congenital muscular dystrophy (FCMD). Acta Neuropathol. 74, 300–306.

Yamamoto, T., Kato, Y., Karita, M., Takeiri, H., Muramatsu, F., Kobayashi, M., Saito, K., Osawa, M., 2002. Fukutin expression in glial cells and neurons: implication in the brain lesions of Fukuyama congenital muscular dystrophy. Acta Neuropathol. 104, 217–224.

Yoshida, A., Kobayashi, K., Manya, H., Taniguchi, K., Kano, H., Mizuno, M., Inazu, T., Mitsuhashi, H., Takahashi, S., Takeuchi, M., Herrmann, R., Straub, V., Talim, B., Voit, T., Topaloglu, H., Toda, T., Endo, T., 2001. Muscular dystrophy and neuronal migration disorder caused by mutations in a glycosyltransferase, POMGnT1. Dev. Cell 1, 717–724.

Zaccaria, M.L., Di Tommaso, F., Brancaccio, A., Paggi, P., Petrucci, T.C., 2001. Dystroglycan distribution in adult mouse brain: a light and electron microscopy study. Neuroscience 104, 311–324.